Chinese Journal of Chemical Engineering 26 (2018) 1003–1011

Contents lists available at ScienceDirect

Chinese Journal of Chemical Engineering

journal homepage: www.elsevier.com/locate/CJChE

Article

Synthesis of activated carbon from spent tea leaves for aspirin removal

Syieluing Wong [1], Yowjeng Lee [1], Norzita Ngadi [1,*], Ibrahim Mohammed Inuwa [2], Nurul Balqis Mohamed [1]

[1] Department of Chemical Engineering, Faculty of Chemical and Energy Engineering, Universiti Teknologi Malaysia, Malaysia
[2] Department of Industrial Chemistry, Kaduna State University, Kaduna, Nigeria

ARTICLE INFO

Article history:
Received 5 July 2017
Received in revised form 7 November 2017
Accepted 8 November 2017
Available online 29 November 2017

Keywords:
Activated carbon
Spent tea leaves
Aspirin
Adsorption
Kinetics
Isotherm

ABSTRACT

Adsorption capacity of activated carbon prepared from spent tea leaves (STL-AC) for the removal of aspirin from aqueous solution was investigated in this study. Preliminary studies have shown that treatment with phosphoric acid (H_3PO_4) increased removal efficiency of STL-AC. Characterizations on STL-AC revealed excellent textural properties (1200 $m^2 \cdot g^{-1}$, 51% mesoporosity), as well as distinctive surface chemistry (1.08 $mmol \cdot g^{-1}$ and 0.54 $mmol \cdot g^{-1}$ for acidic and basic oxygenated groups, $pH_{pzc} = 2.02$). Maximum removal efficiency of aspirin observed was 94.28% after 60 min when the initial concentration was 100 $mg \cdot L^{-1}$, 0.5 g of adsorbent used, pH 3 and at a temperature of 30 °C. The adsorption data were well fitted to the Freundlich isotherm model and obeyed the pseudo-second order kinetics model. The adsorption of aspirin onto STL-AC was exothermic in nature ($\Delta H^{\ominus} = -13.808$ $kJ \cdot mol^{-1}$) and had a negative entropy change, $\Delta S^{\ominus}$ (-41.444 $J \cdot mol^{-1}$). A negative Gibbs free energy, $\Delta G^{\ominus}$ was obtained indicating feasibility and spontaneity of the adsorption process. The adsorption capacity of AC-STL (178.57 $mg \cdot g^{-1}$) is considerably high compared to most adsorbents synthesized from various sources, due to the well-defined textural properties coupled with surface chemistry of STL-AC which favors aspirin adsorption. The results demonstrate the potential of STL-AC as aspirin adsorbent.

1. Introduction

An important concern in the present dispensation is the quality of drinking water especially in the developing nations. The case of underground water pollution is especially more serious, since it includes toxic compounds such as dyes from textile industries, heavy metals, as well as recalcitrant organic compounds from domestic and industrial wastes. In order to ensure the quality of drinking water, various treatment methods have been studied and developed to remove these compounds from domestic and industrial effluent prior to discharge to rivers and streams. Researchers are also aware of certain compounds that are believed to be potential hazards, such as pharmaceutical wastes, to the environmental ecosystems and human body, yet their effects are not fully understood, and their presence in water bodies is not regulated by any water quality law. Although such chemicals might exist in very low concentration in water bodies, bioaccumulation and biomagnification could eventually lead to concentration of these compounds in animals and human body, hence causes noticeable effects, which might be irreversible. Thus, the number of studies on hazardous effects and methods to remove these chemicals, termed as emerging contaminants, is currently rising tremendously [1,2]. PPcPs are categorized as emerging contaminants, as they are able to affect physiological functions, including the endocrine system, of animals and human. One of the difficulties in the treatment of PPcPs in wastewater lies in their ultra-low concentrations, typically in nanogram per liter [3]. However, recent advancements in measuring devices with high precision and sensitivity facilitate the measurements of PPcPs in wastewater.

Several studies demonstrated satisfactory performance of adsorbents derived from biowaste in removal of some common PPcPs, including oxytetracycline [4], paracetamol and caffeine [5], as well as carbamazepine [6]. The used activated carbon can then be regenerated for repeated usage, or incinerated to prevent the movement of pollutants into environment [7].

However, up to date, not much attention is given to aspirin (acetylsalicylic acid, ASA), which is a common over-the-counter drug to reduce fever and to relieve pain. The available studies related to removal of aspirin from wastewater focused on decomposition of the compound through photodegradation [8], advanced oxidation process [9] and microalgal–bacterial system [10]. Adsorption of aspirin from wastewater is considered another potential strategy, due to its economic viability in process design and operation. Applications of size-tunable molecularly imprinted polymer [11], graphene nanoplatelets [12], nanocomposites [13] and commercial activated carbons [14] as adsorbents for aspirin removal from wastewater are explored by few research teams. Despite the large amount of studies on conversion of biowaste to activated carbons [15–18], literature survey indicated only few reports on the use of activated carbon derived from rice hull [19] and biochar derived from southern yellow pine [20] for aspirin removal from simulated wastewater. In view of the potential hazards brought by aspirin as an emerging

* Corresponding author.
E-mail address: norzita@cheme.utm.my (N. Ngadi).

https://doi.org/10.1016/j.cjche.2017.11.004
1004-9541/

contaminant, there is a need to explore the potential of ACs synthesized from cheaper sources of biowaste in removal of aspirin.

Tea is one of the most popular beverages in the world, especially in Asia. Global tea consumption has increased from 2525 million tonnes in 1995 to 5305 million metric tonnes in 2015 [21]. The term tea refers to *Camellia sinensis* leaves which are dried during production. During tea preparation, hot water is used to extract the essence in tea leaves, and spent tea leaves are then discarded. Such waste presents a great potential source for adsorbent preparation. This paper reports adsorption of aspirin onto activated carbon (AC) derived from spent tea leaves *via* chemical activation. Three ACs were prepared using different activating reagents for screening purpose. The AC with the best performance was used to study the effects of contact time, initial adsorbate concentration, adsorbent dosage, pH and temperature of adsorption performance. Adsorption isotherm, kinetic and thermodynamic were also evaluated.

2. Materials and Method

2.1. Synthesis of activated carbon from spent tea leaves (STL-AC)

STL used in this study were obtained from a local restaurant in Johor, Malaysia. STL were boiled repeatedly until the filtered water was clear, then dried in oven for 24 h at 60 °C. The dried STL were then immersed in chemical activating agents at room temperature before dried in oven at 110 °C for 24 h. Three activating agents (K_2CO_3, $ZnCl_2$ and H_3PO_4) were used to study their effects on the AC prepared, and the mass ratio of chemicals to STL was 1:1. After that, the impregnated STL were carbonized at 600 °C for 1 h in an oven. Then, the activated carbon derived from spent tea leaves (STL-AC) was cooled to room temperature and rinsed with distilled water until the pH became neutral (*i.e.* pH 6.5–7.5). The rinsed STL-AC was then dried at 110 °C, ground and sieved to obtained adsorbent in the size of ~500 μm.

2.2. Adsorption of aspirin from aqueous solution using STL-AC

2.2.1. Production of aspirin stock solution and calibration curve

The aspirin stock solution was prepared by mixing aspirin with methanol and distilled water. Analysis of aspirin solutions at 25–500 $mg\cdot L^{-1}$ using a UV–VIS Spectrophotometer (Aquamate v4.60) revealed several characteristic peaks of aspirin, and a calibration curve that relates concentration of aspirin solution to the absorbance at 281 nm was constructed (Supplementary Materials, Fig. S1).

2.2.2. Screening of chemical treated activated carbons

A preliminary study on aspirin removal by chemical activated carbons was performed. For each AC, 0.1 g of the sample was mixed with 50 ml aspirin solution (100 $mg\cdot L^{-1}$) in 125 ml conical flasks. The mixtures were agitated for 60 min at 200 $r\cdot min^{-1}$. After 60 min, the adsorbent was filtered (MN 617, No.4 filter paper) and the concentrations of residual aspirin in the filtered solutions were determined using a UV–VIS spectrophotometer with the help of a calibration curve (Supplementary Materials, Fig. S1). Percentage removals of aspirin by all chemically treated ACs as well as AC without chemical treatment were then calculated using Eq. (1) [22]. The activated carbon with the higher removal performance was selected for further investigation.

$$\text{Percentage removal of aspirin} = \frac{C_o - C_e}{C_o} \times 100\% \quad (1)$$

where C_o and C_e denote the initial and equilibrium concentrations ($mg\cdot L^{-1}$) of aspirin respectively.

2.2.3. Batch adsorption study

Effect of contact time on aspirin adsorption was performed by mixing 50 ml aspirin solution (100 $mg\cdot L^{-1}$, 25 °C) with 0.1 g of STL-AC in a conical flask. The mixture was agitated at 200 $r\cdot min^{-1}$ for 180 min. Samples were collected from the mixture for UV–Vis analysis at every 5 min for the first 30 min, then every 10 min for the rest of the experiment. The optimum contact time was then selected based on adsorption data and used in the next set of experiment, where adsorption study was performed using a series of conical flasks containing aspirin solutions in a concentration range of 100–500 $mg\cdot L^{-1}$. After that, the influence of pH on adsorption was studied by adjusting the initial pH value of aspirin solutions from 2 to 11 using 0.1 $mol\cdot L^{-1}$ NaOH and 0.1 $mol\cdot L^{-1}$ HCl, while adsorption thermodynamics was studied by conducting the experiment at 30 °C, 40 °C and 50 °C. The amount of aspirin adsorbed to STL-AC adsorbent at equilibrium, q_e ($mg\cdot g^{-1}$), was calculated using Eq. (2), while aspirin adsorbed at time t, q_t ($mg\cdot g^{-1}$) was calculated using Eq. (3) [5].

$$q_e = \frac{(C_o - C_e)V}{W} \quad (2)$$

$$q_t = \frac{(C_o - C_t)V}{W} \quad (3)$$

where

C_o is the initial concentration of aspirin, $mg\cdot L^{-1}$,
C_e and C_t are the concentration of aspirin at equilibrium and at time t, respectively, $mg\cdot L^{-1}$,
V is the volume of aspirin solution, L, and
W is the mass of STL-AC adsorbent used, g.

2.3. Characterizations of STL-AC

Several characterization tests were carried out on fresh and used STL-AC. A nitrogen adsorption–desorption test was carried out on the samples using Micromeritic Pulse Chemisorb 2705 at 77 K according to the multi-point BET method to determine the surface area and pore size distribution of the adsorbents. Field Emission Scanning Electron Microscopy (SUPRA™ 35VP Carl Zeiss GEMINI®) was used to study the morphologies of the samples. The samples were coated with an extremely thin gold–palladium layer to create an electrically conductive film prior to the analysis.

The surface chemistry of STL-AC was studied using an FTIR Spectrophotometer (Perkin-Elmer Spectrum ONE) in the region of 400–4000 cm^{-1}. The KBr method was applied in the sample preparation. The spectrum of samples was compared with standard spectra from database in order to identify the functional groups on the adsorbent. The acidic and basic functional groups on STL-AC surface were determined through Boehm titration according to the methods described by Tran *et al.* [23] and Song *et al.* [24]. The underlying principle associated with this method is that the acidic groups that present on the adsorbent surface consist carboxylic, phenolic and lactonic groups. Among these groups, $NaHCO_3$ reacts with only carboxylic groups, while Na_2CO_3 reacts with carboxylic and lactonic groups, and NaOH reacts with all acidic groups. All the solutions used in this test were prepared using boiled distilled water to minimize the effect of dissolved CO_2 as discussed by Goertzen *et al.* [25]. To begin the analysis, 0.5 g of adsorbent was added to four conical flasks (50 ml), each containing 25 ml of 0.05 $mol\cdot L^{-1}$ NaOH, Na_2CO_3, and $NaHCO_3$ solutions respectively. The flasks were sealed with parafilm and shaken for 48 h at room temperature (25 °C). The adsorbents were then filtered off the solutions, and 10 ml of aliquots was obtained from each filtered solutions. The aliquots were acidified by 20 ml of HCl solutions (0.05 $mol\cdot L^{-1}$) on aliquots of the reaction bases NaOH as well as $NaHCO_3$, while 30 ml of HCl solution (0.05 $mol\cdot L^{-1}$) was added to the aliquot of the reaction base Na_2CO_3. Methyl orange indicator was used to determine the titration endpoint. Point of zero charge (pH_{pzc}) of STL-AC was determined according to the solid addition method [26,27]. The test protocol involved preparation of NaCl solution (0.01 $mol\cdot L^{-1}$) from boiled distilled water to

minimize the influence of dissolved CO_2. Then, six test samples containing 50 ml of NaCl solution in tightly closed bottles with an initial pH of 2–12 (adjusted using 0.1 mol·L^{-1} NaOH and 0.1 mol·L^{-1} HCl solutions) were prepared. This was followed by the addition of 0.15 g STL-AC to each container, and the bottles were allowed to equilibrate through mixing in a shaker set at 150 r·min^{-1}. After 24 h, the final pH of each sample was recorded. A graph of final pH against initial pH was plotted for all samples, and the point of intersection between the plot with straight line $y = x$ represents pH_{pzc} for STL-AC.

3. Results and Discussion

3.1. Effect of activating agents on the adsorbent performance

Chemical activation is preferred over physical activation in adsorbent synthesis due to simplicity and lower temperature requirement [28]. The use of different chemical activating agents results in different morphology and surface chemistry of the adsorbents, hence affecting the adsorption performance, thus selection of suitable activating agent is crucial. In this study, $ZnCl_2$, H_3PO_4 and K_2CO_3 were used in the treatment of STL prior to activation at 600 °C. A simple screening test was conducted to determine the best chemical activating agent among the chemical activated STL-AC, as well as STL-AC synthesized *via* physical treatment only and raw STL, based on the aspirin removal performances from aqueous solution. The comparison, as shown in Table 1, revealed the STL-AC synthesize *via* chemical treatments (31%–68%) possess higher removal efficiencies than STL-AC without chemical treatment (~13%) as well as raw STL (~5%). H_3PO_4 is the most suitable agent to be used in chemical activation of STL-AC, as evidenced by 68.04% of adsorption performance after the adsorption process for 60 min. Thus, the H_3PO_4 was selected as the chemical activating agent for the adsorbent.

Table 1
Screening test of raw spent tea leaves and different activated carbons in removal of aspirin in aqueous solutions

Type of adsorbent	Removal efficiency/%
Raw STL	5.79
STL-AC without chemical treatment	13.41
STL-AC treated with H_3PO_4	68.04
STL-AC treated with $ZnCl_2$	49.83
STL-AC treated with K_2CO_3	31.29

3.2. Characterization of STL-AC

3.2.1. Fourier Transform Infrared (FTIR)

The FTIR spectra of the adsorbents are presented in Fig. 1 and Table 2. The strong and broad band at 3442 cm^{-1} as shown in Fig. 1 is attributed to the stretching vibration of the hydroxyl group [29]. The peak at 1628 cm^{-1} was assigned to the asymmetric stretching vibration of C═O [17], while the peak at 1381 cm^{-1} represents the symmetric bending of CH_3 [30,31]. A similar spectrum is observed for used STL-AC after aspirin adsorption, with slight shift of the wavelengths observed for the peaks.

Table 2
FTIR spectral characteristics of STL-AC before adsorption and after adsorption of aspirin in aqueous solution

Frequency/cm^{-1}		Functional group
Before adsorption	After adsorption	
3442	3442	Bonded —OH group
1628	1631	C═O stretching
1381	1384	Symmetric bending of CH_3

3.2.2. Boehm titration and point of zero charge (pH_{pzc})

Information on oxygenated groups present on the adsorbent surface reveals the possible interactions between adsorbent and adsorbate. In general, acidic and basic groups co-exist on AC surface, and the difference in their abundance determines the net charge on the adsorbent surface. Introduction of acidic oxygenated groups, including carboxyl, lactonic and phenolic groups, onto AC *via* chemical activation using acidic reagent is reported in many studies as indicated in Table 3. Activation of AC precursor at high temperature (>750 °C) is reported to cause decomposition of acidic oxygenated groups leading to higher number of basic oxygenated group compared to acidic ones [32]. STL-AC synthesized in this study contains almost equal amount of lactonic and phenolic, as well as basic oxygenated groups, as listed in Table 3. The presence of phenolic group is in agreement with the —OH groups in Fig. 1. On the other hand, the presence of carboxylic group is not detected according to titration result, the C═O group shown in FTIR spectra could be assigned to only lactonic group [23]. The total amount of acidic and basic functional groups on STL-AC is comparable to the ACs prepared in other works. Nevertheless, the exact test procedure steps used by all researchers are slightly different from one another (especially on the stirring time and volume of aliquots used during titration) although these procedures are created based on the same principle. Thus, direct comparison on the amount of surface functional groups may not reflect the true differences in surface chemistry of these adsorbents. Among the acidic oxygenated groups, phenolics are able to form hydrogen bonding with aspirin molecules as indicated by Bernal *et al.* [33]. In addition, basic oxygenated groups on STL-AC form electrostatic interaction with anions formed by deprotonated aspirin molecules. Therefore, the surface chemistry of STL-AC favors adsorption of aspirin in both neutral and anionic forms.

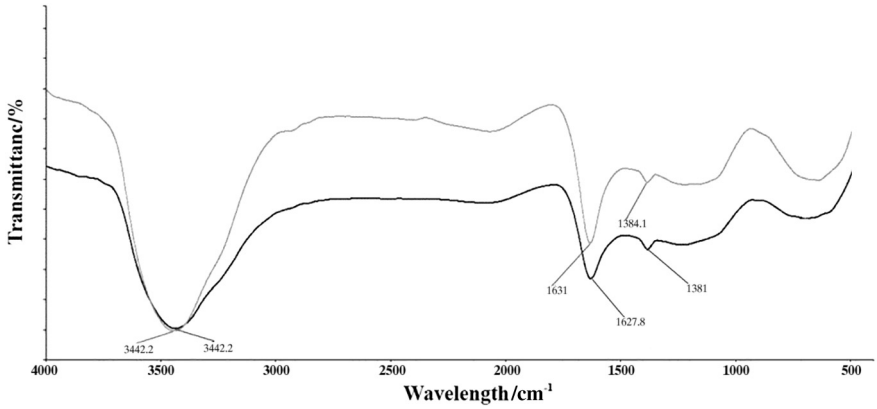

Fig. 1. FTIR spectra of STL-AC before and after adsorption of aspirin in aqueous solution.

Table 3
Amount of surface functional groups on ACs prepared from different precursors and methods

Precursor and preparation method	Functional groups/mmol·g^{-1}					pH_{pzc}	Ref.
	Carboxylic	Lactonic	Phenolic	Acid	Basic		
H_3PO_4-STL-AC	0.00	0.50	0.58	1.08	0.54	2.02	This study
Tea waste (CH_3CO_2K/800 °C, N_2)	0.341	0.022	1.211	1.574	2.558	7.2	[35]
Tea waste (H_3PO_4, microwave/N_2, 450 °C)	0.131	0.651	0.050	0.832	0.110	N.A.	[36]
Spent tea leaves (H_3PO_4/600 °C, N_2)	1.27	0.59	1.25	3.11	0.13	4.6	[37]
Tea waste ($ZnCl_2$/N_2, 700 °C)	0.98	0.57	0.95	2.50	–	6.5	[38]
Rice husk (300 °C/H_3PO_4/600 °C, N_2)	0.45	0.43	0.44	1.32	0.43	N.A.	[39]
Olive stone (H_3PO_4/380 °C, N_2)	1.45	0.05	0.70	2.20	0.00	4.00	[26]
Weeds (500 °C, N_2/HNO_3)	0.610	0.724	0.940	2.274	0.578	4.00	[40]
Plantain fruit stem (400 °C/HNO_3/400 °C)	0.09	0.08	0.03	0.20	1.62	N.A.	[41]
AF fruit waste (700 °C, N_2/750 °C, H_2O)	1.34	0.21	0.15	1.7	3.3	N.A.	[32]
Bamboo (H_3PO_4/500 °C, H_2O + N_2)	1.454	0.210	0.140	1.804	–	2.41	[34]

Another important property of adsorbents is the value of pH_{pzc}, as such property influences the adsorbent–adsorbate interaction under different pH, especially when ionization of adsorbate is significant. When immersed in solution with pH less than pH_{pzc}, the adsorbent is surrounded with positive charge, and the reverse is true. Most of the adsorbents synthesized in literature have pH_{pzc} values slightly less than 7, due to the higher quantity of acidic oxygenated groups on the adsorbent surface. The same reasoning applies on STL-AC, which have pH_{pzc} of 2.20, due to the use of phosphoric acid as activating agent. Similarly, AC synthesized from bamboo *via* phosphoric acid treatment by Santana *et al.* [34] also exhibited very low pH_{pzc}. However, more detailed studies are needed to study on effects of activating agent and surface functional groups on the pH_{pzc} values of the adsorbents synthesized from biowaste.

3.2.3. Brunauer–Emmett–Teller (BET) analysis

BET analysis was conducted to determine the characteristics of STL-AC in terms of surface area, as well as pore volume and size. The N_2 adsorption and desorption isotherm at 77 K for STL-AC is shown in Fig. 2. Type IV isotherm was observed according to the International Union of Pure and Applied Chemistry (IUPAC) classification. Adsorbents with type IV isotherm are characterized with mesoporous structure. At lower pressure region, the adsorption isotherm is similar to Type II isotherm, which explains the formation of a monolayer followed by a multilayer of adsorbates on the adsorbent. The presence of hysteresis loop indicates capillary condensation in the mesoporous surface [42]. The isotherm observed for this adsorbent is similar to those of commercial activated carbons [43].

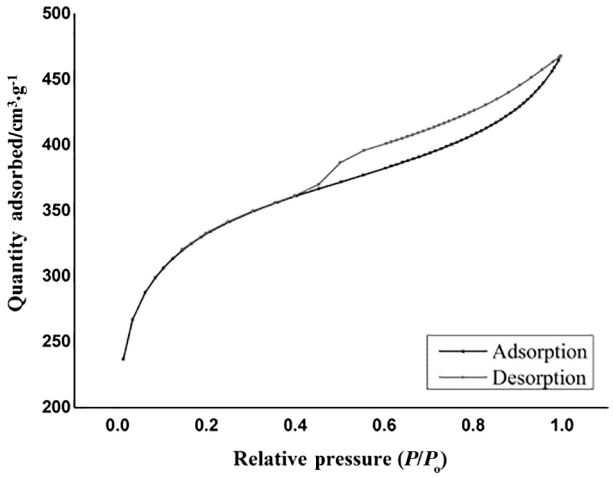

Fig. 2. N_2 adsorption and desorption profile for STL-AC.

The BET surface area of STL-AC (1200 $m^2 \cdot g^{-1}$) is comparable to the commercial activated carbon mentioned in Table 4. When compared with AC derived from spent tea leaves prepared *via* microwave activation [44], AC was found to be about twice the value for the BET total surface area and total pore volume. Another distinctive feature of STL-AC is the high porosity. The micropore and mesopore surface areas were 694.07 $m^2 \cdot g^{-1}$ and 362.29 $m^2 \cdot g^{-1}$, respectively. In addition, mesopore volume (0.370 $cm^3 \cdot g^{-1}$) contributed to about 51% of its total pore volume, indicating the high mesoporosity of the adsorbent [45]. The average pore size for STL-AC measured was about 2.4 nm, which was slightly larger than the micropore size (<2 nm). This is in contrast with other chemical or physical activated tea waste or spent tea leaves listed in Table 4, which have average pore sizes in between 2 nm and 3 nm. Therefore, it is concluded that STL-AC synthesized *via* H_3PO_4 treatment possesses superior textural properties due to pyrolytic decomposition and cross-link structure between the phosphate and fragments present in biomass [46].

3.2.4. Field emission scanning electron microscopy (FESEM)

The surface morphology of STL-AC adsorbent before and after aspirin adsorption was investigated using FESEM. Fig. 3(a) clearly depicts the irregular macropores and mesopores in fresh adsorbent which are composed of a tunnel porous shape. Non-homogenous micropores were observed on the inner surface of the porous tunnel. The outer surface of the adsorbent was rough and some cracks can be seen. The porous characteristic was hardly observed on the used adsorbent (Fig. 3(b)), as the pores were filled up. The significant changes observed indicated aspirin was adsorbed onto STL-AC.

3.3. Effect of various parameters in adsorption

3.3.1. Effect of contact time

The effect of contact time on aspirin removal by STL-AC is shown in Fig. 4. The aspirin adsorption rate rose sharply for the first 30 min and then levels up at 60 min onward. This is the result of concentration gradient created between aspirin molecules in aqueous solution and the adsorbent surface, as well as the presence of abundant active sites on the surface of the adsorbent at the start of the adsorption process. As time progresses, the remaining vacant sites on the adsorbent surface decreased, resulting in the observed reduction of adsorption rate. This is due to repulsive forces between the solute molecules on the solid phase and in the bulk liquid phase [50].

3.3.2. Effect of initial aspirin concentration

Fig. 5 reveals that the amount of aspirin adsorbed (q_e) increased with initial aspirin concentration, whereas the removal efficiency of aspirin showed an opposite trend. The amount of aspirin adsorbed increased from 35 mg·g^{-1} to 119.56 mg·g^{-1} while the removal

Table 4
Comparison on textural properties of STL-AC with other adsorbents

Adsorbent	BET total surface area/$m^2 \cdot g^{-1}$	Micropore surface area/$m^2 \cdot g^{-1}$	Mesopore surface area/$m^2 \cdot g^{-1}$	Total pore volume/$cm^3 \cdot g^{-1}$	Micropore volume/$cm^3 \cdot g^{-1}$	Mesopore volume/$cm^3 \cdot g^{-1}$	Average pore diameter/nm	Ref.
H_3PO_4-STL-AC (1:1 ratio, 600 °C, 1 h)	1202.84	694.07	362.29	0.720	0.290	0.370	2.395	Present study
$ZnCl_2$-AC-TW (1:2 ratio, 700 °C, 4 h)	706.00	629.00	77.00	0.369	0.324	0.045	2.090	[47]
$ZnCl_2$-AC-TW (1:1 ratio, 700 °C, 4 h)	1066.00	641.00	425.00	0.580	0.337	0.243	2.180	
K_2CO_3-AC-TW (1:2 ratio. 900 °C, 1 h)	609.00	–	–	0.390	0.157	0.233	–	[48]
K_2CO_3-AC-TW (1:1 ratio. 900 °C, 1 h)	1722.00	–	–	0.946	0.570	0.376	–	
K_2CO_3-AC-TW (2:1 ratio. 900 °C, 1 h)	1597.00	–	–	0.975	0.416	0.559	–	
Microwave activated tea waste (5 min, 800 W, 2450 MHz)	537.40	–	–	0.400	–	–	2.827	[44]
Pristine AC from Sigma-Aldrich①	1265.00	698.00	567.00	1.100	0.220	0.820	–	[49]
Bologna-based Polichimica AC①	1431.00	1096.00	335.00	0.840	0.260	0.490		

① Commercial activated carbon.

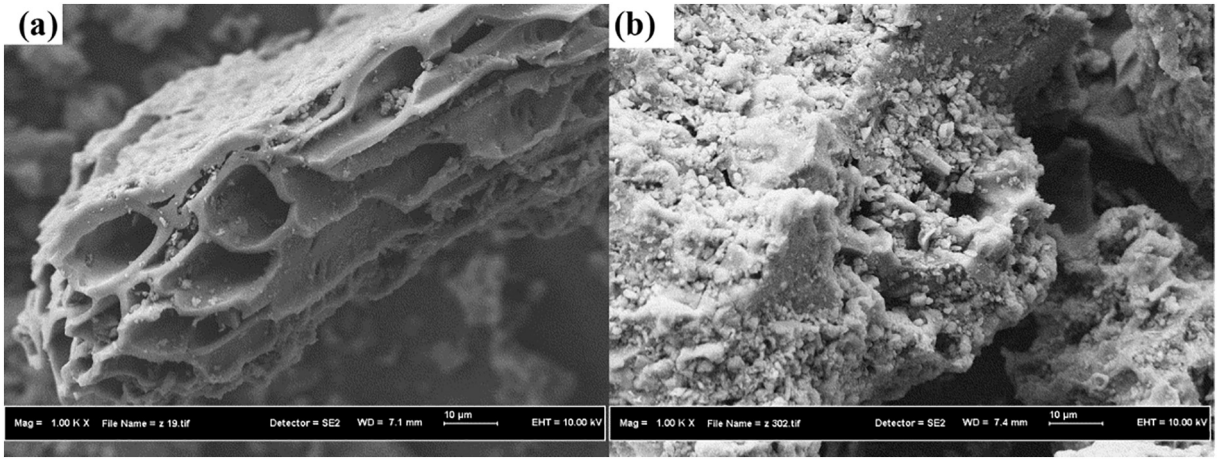

Fig. 3. Field emission scanning electron microscopy image of STL-AC (a) before adsorption and (b) after adsorption of aspirin in aqueous solution.

efficiency decreased from 71.89% to 47.23%. Increasing initial concentration led to larger mass transfer driving force of the adsorbate onto the adsorbent, hence resulting in higher aspirin adsorption [51]. When the initial concentration of aspirin used was 400 $mg \cdot L^{-1}$, the amount of aspirin adsorbed, q_e was slightly lower compared to that in 500 $mg \cdot L^{-1}$, as saturation limit was achieved at the surface of adsorbent. The optimum initial aspirin concentration used for further study was 100 $mg \cdot L^{-1}$ which is due to its higher removal efficiency.

3.3.3. *Effect of adsorbent dosage*

Fig. 6 shows that the removal efficiency of aspirin increased by 20% when the adsorbent dosage increased from 0.1 g to 0.5 g. Increasing amount of adsorbent dosage provides more accessible binding sites. However, the removal efficiency was the highest when 0.5 g of adsorbent was used (which is 90.59%), and further increase in adsorbent dosage had little improvement. This is probably due to agglomeration of exchanger particles resulting in overlapping of active sites and reducing

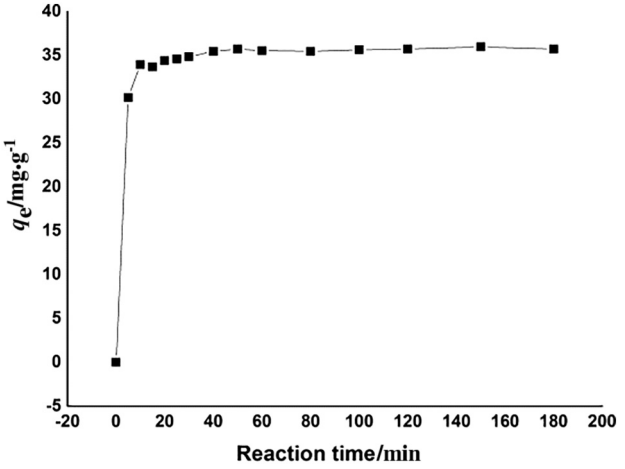

Fig. 4. Effect of contact time on aspirin adsorption by STL-AC. (100 $mg \cdot L^{-1}$ aspirin in solution, 0.1 g adsorbent, 180 min reaction time, room temperatures, pH 3.28 which is the original pH of aspirin solution).

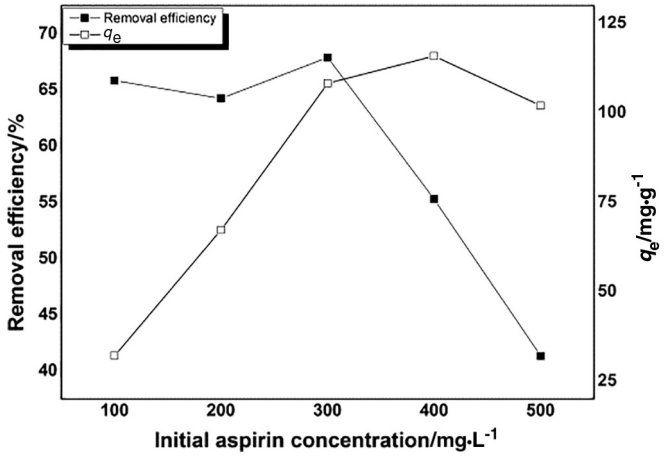

Fig. 5. Effect of initial aspirin concentration on aspirin adsorption by STL-AC. (0.1 g adsorbent, 60 min reaction time, room temperature, pH 3.4 which is the original pH of aspirin solution).

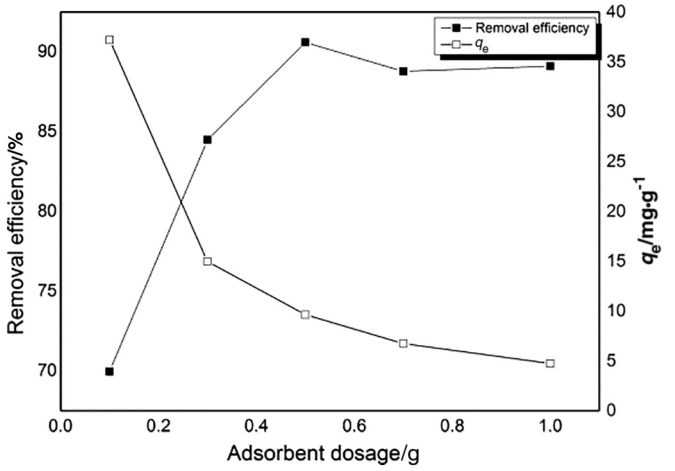

Fig. 6. Effect of STL-AC dosage on aspirin adsorption by STL-AC. (100 mg·L^{-1} aspirin solution, 60 min reaction time, room temperature, pH 3.37 which is the original pH of aspirin solution).

the effective surface area on the adsorbent [52]. In contrast, the adsorption capacity decreased with adsorbent dosage, due to the increment of surface vicinity and availability of active binding sites, thus some sites were unoccupied [53]. Based on Fig. 6, 0.5 g of adsorbent was selected as the optimum dosage for aspirin absorption.

3.3.4. Effect of pH

Fig. 7 conveys that the removal efficiency and amount of aspirin adsorbed decreased with pH value. The highest aspirin removal efficiency was recorded at pH 3 (about 94%). The adsorption performance reduced with pH, and 68.62% removal efficiency was observed at pH 11. Such trend is related to pH_{pzc} of STL-AC (2.02). Thus, the adsorbent is negatively charged below pH 2. On the other hand, aspirin is known as a weak acid ($pK_a = 3.5$), which undergoes partial deprotonation in water to produce anions. Following the increase of pH, the adsorbent tends to be more negatively charged, hence adsorption of deprotonated aspirin species is hindered due to the electrostatic repulsion force [33]. This translates to higher energy requirement for the adsorbate–adsorbent interactions [33]. In addition, there was also competition between hydroxide (OH^-) and the aspirin anions for the positively charged adsorption sites at high pH [13]. In view of the above statements, adsorption is less favorable above pH 2.02 if electrostatic attraction between adsorbates and adsorbents is the sole factor in mechanism. However, in view of the high adsorption performance of aspirin at pH 3, it is reasonable to deduce that the electrostatic attraction is not the most significant factor in adsorption mechanism (due to the low dissociation of aspirin molecules). Instead, interactions between basic oxygenated groups as well as phenolic groups (as explained in Section 3.2.2) on adsorbent surface and aspirin molecules could be more important in this case.

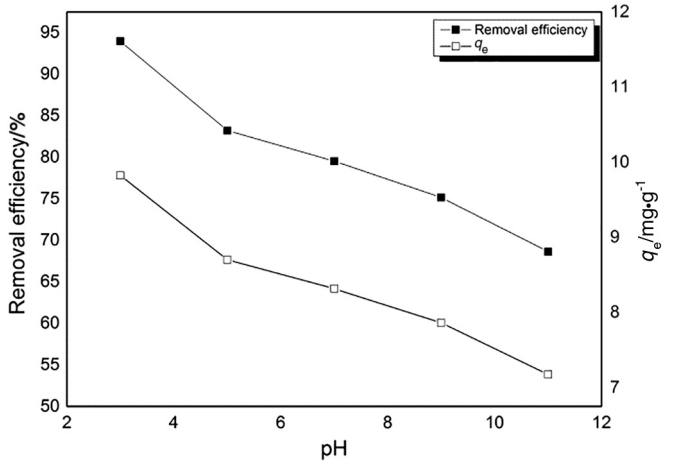

Fig. 7. Effect of pH on aspirin adsorption by STL-AC (100 mg·L^{-1} aspirin solution, 0.5 g adsorbent, 60 min reaction time, room temperature).

3.3.5. Effect of temperature

Fig. 8 shows that the adsorption of aspirin by STL-AC was insensitive to temperature. Only a slight decrease in removal efficiency and amount of aspirin adsorbed was observed at elevated temperature. The same result was reported in the study investigated by Mphahlele *et al.* [13]. The decreased in amount of aspirin adsorbed at higher temperature is due to the exothermic nature of the adsorption process.

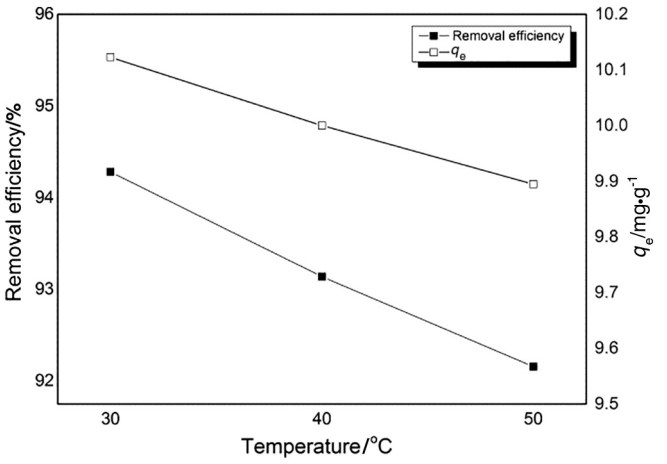

Fig. 8. Effect of temperature on aspirin adsorption by STL-AC (100 mg·L^{-1} aspirin solution, 0.5 g adsorbent, 60 min reaction time, pH = 3).

3.4. Adsorption isotherm evaluation

The study on adsorption isotherm provides information on distribution of adsorbate molecules between liquid and solid phases at equilibrium state. Selection of appropriate isotherm model is crucial for design and operation purposes [54]. Four adsorption isotherm models were used in data fitting process. The Langmuir isotherm model assumes occurrence of adsorption on homogeneous sites on the adsorbent surface, and only a single adsorbate layer is formed [26]. On the other hand, the Freundlich model is used to describe multilayer adsorption with non-uniform distribution of adsorption heat and affinities over the heterogeneous surface [55]. The Temkin model assumes that interactions between adsorbents and adsorbates lead to reduction of the adsorption energy with surface coverage [26], while the Dubinin–Radushkevich model is used based on consideration that adsorption surface is heterogeneous, and micropore filling takes place based on free adsorption enthalpy that is not constant, and is able to affect free adsorption enthalpy [56]. The linearized Langmuir, Freundlich, Temkin and Dubinin–Radushkevich isotherm models are expressed in Eqs. (4), (5), (6) and (7) respectively [22,57,58].

$$\frac{C_e}{q_e} = \frac{1}{q_m K_L} + \frac{C_e}{q_e} \tag{4}$$

$$\lg q_e = \lg K_F + \left(\frac{1}{n}\right) \lg C_e \tag{5}$$

$$q_e = B \ln K_T + B \ln C_e \tag{6}$$

$$\ln q_e = \ln Q_s - Be^2 \quad (7)$$

where

C_e (mg·L^{-1}) is the equilibrium concentration of adsorbate,
q_m (mg·g^{-1}) is the maximum adsorption capacity per unit mass of adsorbent,
q_e (mg·g^{-1}) is the adsorption capacity at equilibrium,
K_L (L·mg^{-1}) is the Langmuir constant,
K_F (mg·g^{-1}·L$^{-1/n}$·mg$^{-1/n}$) is the Freundlich constant,
n (dimensionless) is the Freundlich intensity,
B (J·mol^{-1}) is a constant related to heat of adsorption, and
K_T (L·g^{-1}) is the equilibrium binding constant.

The linearized plots for Langmuir, Freundlich, Temkin and Dubinin–Radushkevich are shown in Fig. S2 (Supplementary Materials). The calculated constants in the four isotherm equations along with the respective R^2 values are listed in Table 5. The R^2 value for the Freundlich isotherm model is the largest among all the fitted plots, therefore the experimental data is better fitted to the Freundlich isotherm, and multilayer adsorption takes place during the process. Similar results were also reported by Rakic *et al.* [14] and Mphahlele *et al.* [13]. The magnitude of the exponent (1/n) indicates the favorability of the heterogeneous adsorption. The adsorption is favorable when $n > 1$ [59]. In the present study, the value for n is 1.75 as shown in Table 5, indicating the favorability of the adsorption of aspirin onto STL-AC.

Table 5
The adsorption isotherm parameters for adsorption of aspirin onto STL-AC

Isotherm model	Parameter	Value
Langmuir isotherm	Q_{max}/mg·g^{-1}	178.57
	K_L/L·g^{-1}	8.44
	R^2	0.9763
Freundlich isotherm	K_F/mg·g^{-1}	5.40
	n	1.75
	R^2	0.9813
Temkin	β	38.382
	R^2	0.9761
Dubinin–Radushkevich (D–R)	k_d	8×10^{-10}
	Q_m	79.82
	E	25000.00
	R^2	0.01

3.5. Adsorption kinetic examination

The adsorption kinetic of aspirin onto STL-AC was evaluated using pseudo-first order, pseudo-second order and intraparticle diffusion kinetic models (Supplementary Materials, Fig. S3), and the linearized models are shown in Eqs. (8), (9), and (10) [5,22]. The value of correlation coefficient, R^2 and other parameters acquired form the plots are tabulated in Table 6.

$$\lg (q_e - q_t) = \lg q_e - k_1 t \quad (8)$$

Table 6
Adsorption kinetic parameters for the adsorption of aspirin

Kinetic model	Parameter	Value
Pseudo-first order model	k_1/min^{-1}	0.126
	q_e/mg·g^{-1}	12.64
	R^2	0.8190
Pseudo-second order model	k_2/g·mg^{-1}·min^{-1}	0.0279
	q_e/mg·g^{-1}	36.23
	R^2	0.9999
Intraparticle diffusion model	k_{int}	0.7869
	C	30.283
	R^2	0.722

$$\frac{t}{q_t} = \frac{1}{k_2 q_e^2} + \left(\frac{1}{q_e}\right) t \quad (9)$$

$$q_t = k_{int} t^{0.5} + C \quad (10)$$

where

q_e and q_t (mg·g^{-1}) are the adsorption capacities at equilibrium and at time t respectively,
k_1 and k_2 (min^{-1}) are pseudo-first and pseudo-second order rate constants respectively, and
k_{int} (mg·g^{-1}·min$^{0.5}$) is the rate constant of adsorption capacity.

From Fig. S3(a), the R^2 value for the pseudo-first order kinetic model is 0.819, and a large difference is observed between experimental equilibrium adsorption capacity (q_e = 35.526 mg·g^{-1}) and theoretical value obtained from the model. These findings indicate that the pseudo-first order kinetic model is poorly fitted to the experimental data. On the other hand, good fitting of adsorption data to the pseudo-second order model is observed in Fig. S3(b), as evidenced by an R^2 value of 0.9999. The theoretical q_e value obtained *via* this model (36.23 mg·g^{-1}) is also closer to the experimental value. These evidences suggest that the experiment data are well represented by pseudo-second order kinetics. Therefore, it can be said that the adsorption is dominated by chemisorption as discussed in many works in literature [60], although more studies are needed to obtain conclusive evidence on relationship between the pseudo-second order model and chemisorption process [61]. Adsorption process defined by the pseudo-second order model is also characterized by an increase in the adsorption rate with initial aspirin concentration, due to increasing driving force at high concentration [56,62].

In order to gain insight on the mechanism and rate controlling step affecting the adsorption kinetic, it is necessary to fit the experiment data to the intraparticle diffusion model (Eq. (10)). The value of intercept (C) obtained from the plot reflects the boundary layer thickness, thus the larger the intercept value, the greater the contribution of the surface sorption in the rate-controlling step. On the other hand, the adsorption process is said to be controlled solely by intraparticle diffusion if the linear plot passes through the origin, which means the intercept value equals to zero. In this study, the linear plot does not pass through the origin [Supplementary Materials, Fig. S3(c)], thus intraparticle diffusion is not the only rate controlling step.

3.6. Adsorption thermodynamic analysis

Thermodynamic analysis was performed to study the spontaneity of the adsorption process (ΔG^o), as well as its nature of enthalpy (ΔH^o) and entropy change (ΔS^o). Eqs. (11) and (12) were utilized to determine the magnitude of thermodynamic parameters such as changes in standard Gibbs free energy (ΔG^o), standard enthalpy (ΔH^o), and standard entropy (ΔS^o) [63,64]. Using the experimental data in the study of temperature effect on adsorption process, a graph of ln K_{eq} was plotted against 1/T (Supplementary Materials, Fig. S4). Based on the slope and intercept of the plot, the enthalpy and entropy changes are calculated and listed in Table 7.

$$\Delta G^o = -RT \ln K_L \quad (11)$$

Table 7
Thermodynamic parameters for adsorption of aspirin in aqueous solution onto STL-AC

Pharmaceutical compound	Enthalpy change, $H^\ominus$/kJ·mol^{-1}	Entropy change, $S^\ominus$/J·mol^{-1}	Gibbs free energy, $\Delta G^\ominus$/kJ·mol^{-1}		
			303.15 K	313.15 K	323.15 K
Aspirin	−13.808	−41.444	−1.259	−0.795	−0.433

$$\ln K_L = \frac{\Delta S^{\Theta}}{R} - \frac{\Delta H^{\Theta}}{RT} \quad (12)$$

where

R is a gas constant, 8.314 $J \cdot mol^{-1} \cdot K^{-1}$,

T (K) is the absolute temperature, and

K_L is an equilibrium constant.

From Fig. S4, the enthalpy change (ΔH^o) for aspirin adsorption is -13.808 $kJ \cdot mol^{-1}$. The negative value of ΔH^o indicates the exothermic nature of the adsorption process, which explains the decrease in adsorption capacity at higher temperature. The entropy change (ΔS^o) of the adsorption process calculated from the plot was -41.444 $J \cdot mol^{-1}$. This negative value indicated a decrease in randomness at the STL-AC/aspirin solution interface. Moreover, the negative value indicated that the aspirin adsorption onto STL-AC may be attributed to the decrease in the degree of freedom of aspirin molecules. The negative value of ΔG^o obtained indicated that the adsorption of aspirin onto STL-AC is feasible and spontaneous. The Gibbs energy value (ΔG^o) decreases with temperature as shown in Table 7, which is related to higher adsorption capacity [12].

3.7. Adsorption performance of STL-AC compared to other adsorbents

As mentioned in the Introduction section, there are very few reports on the adsorption of aspirin from simulated wastewater. As shown in Table 8, the adsorption capacity of AC-STL synthesized in this study is far higher than most adsorbents synthesized *via* different sources and methods, and is comparable to AC derived from rice hull. The high performance of STL-AC is most probably due to the excellent textural properties (high surface area, as well as pore volume and diameter) together with the presence of surface oxygenated groups that interact with the adsorbate molecules *via* hydrogen bonding and electrostatic attraction (especially at low pH). The comparison also illustrates the superior property of AC synthesized from biowaste in aspirin adsorption. Combined with lower cost related to precursor as well as simpler preparation method compared to other types of adsorbents, there is a huge potential of AC from biowaste to be applied in wastewater treatment process.

Table 8
Comparison of adsorption results with other adsorbents in literature

Adsorbents	Adsorption capacity/$mg \cdot g^{-1}$	Reference
AC derived from rice hull (H_3PO_4/500 °C)	178.89	[19]
AC derived from spent tea leaves (H_3PO_4/600 °C)	178.57	This study
Fe/N-CNT/β-cyclodextrin nanocomposites	71.9	[13]
Graphene nanoplatelets	12.98	[12]
Size-tunable molecularly imprinted polymer	0.03	[11]

4. Conclusions

Adsorption of aspirin from aqueous solution onto STL-AC was investigated. The AC synthesized *via* H_3PO_4 activation presented the best adsorption performance among the potential adsorbents. Such adsorbent is characterized by high surface area and pore properties, as well as considerable amount of acidic and basic oxygenated groups. The highest removal efficiency of aspirin observed was 94.28% after 60 min when the initial concentration was 100 $mg \cdot L^{-1}$, 0.5 g of adsorbent used, pH 3 and at a temperature of 30 °C. Adsorption isotherm analysis revealed that the adsorption experiment data fitted well to the Freundlich isotherm model with n value greater than 1. This indicates that the adsorption process is favorable. For the kinetic study, adsorption of aspirin onto STL-AC fitted well to the pseudo-second order kinetic model. Thermodynamic analysis showed that the adsorption is exothermic in nature. The negative entropy value (ΔS^o) indicated a decrease in randomness at the STL-AC/aspirin solution interface during the adsorption process. Lastly, the negative value of ΔG^o obtained, indicated that the adsorption of aspirin onto STL-AC is feasible and spontaneous. Based on the characterization results on STL-AC and modeling result on adsorption data, the excellent adsorption property of aspirin onto STL-AC is most likely attributed to the adsorbent surface and pore properties together with interactions between surface oxygenated groups with the adsorbate molecules.

Acknowledgments

This work was supported by Malaysia's Ministry of Higher Education's Fundamental Research Grant Scheme (FRGS, grant number 4F872) as well as Research University grant (GUP, grant number 17H65). The main author, Wong Syie Luing, is also thankful for the support from Universiti Teknologi Malaysia in the form of Post-Doctoral Fellowship Scheme for the Project: "Catalytic Cracking of Low Density Polyethylene Waste to Liquid Fuels in Fixed Bed Reactor".

Supplementary Material

Supplementary data to this article can be found online at https://doi.org/10.1016/j.cjche.2017.11.004.

References

[1] N. Chaukura, W. Gwenzi, N. Tavengwa, M.M. Manyuchi, Biosorbents for the removal of synthetic organics and emerging pollutants: Opportunities and challenges for developing countries, *Environ. Dev.* 19 (2016) 84–89.
[2] W. Gwenzi, N. Chaukura, C. Noubactep, F.N.D. Mukome, Biochar-based water treatment systems as a potential low-cost and sustainable technology for clean water provision, *J. Environ. Manag.* 197 (2017) 732–749.
[3] E. Archer, B. Petrie, B. Kasprzyk-Hordern, G.M. Wolfaardt, The fate of pharmaceuticals and personal care products (PPCPs), endocrine disrupting contaminants (EDCs), metabolites and illicit drugs in a WWTW and environmental waters, *Chemosphere* 174 (2017) 437–446.
[4] Y. Kan, Q. Yue, D. Li, Y. Wu, B. Gao, Preparation and characterization of activated carbons from waste tea by H_3PO_4 activation in different atmospheres for oxytetracycline removal, *J. Taiwan Inst. Chem. Eng.* 71 (2017) 494–500.
[5] P.S. Thue, E.C. Lima, J.M. Sieliechi, C. Saucier, S.L.P. Dias, J.C.P. Vaghetti, F.S. Rodembusch, F.A. Pavan, Effects of first-row transition metals and impregnation ratios on the physicochemical properties of microwave-assisted activated carbons from wood biomass, *J. Colloid Interface Sci.* 486 (2017) 163–175.
[6] V. Calisto, G. Jaria, C.P. Silva, C.I. Ferreira, M. Otero, V.I. Esteves, Single and multicomponent adsorption of psychiatric pharmaceuticals onto alternative and commercial carbons, *J. Environ. Manag.* 192 (2017) 15–24.
[7] A. Chouchene, M. Jeguirim, G. Trouve, Biosorption performance, combustion behavior, and leaching characteristics of olive solid waste during the removal of copper and nickel from aqueous solutions, *Clean Techn. Environ. Policy* 16 (5) (2014) 979–986.
[8] C.L. Bianchi, B. Sacchi, S. Capelli, C. Pirola, G. Cerrato, S. Morandi, V. Capucci, Microsized TiO_2 as photoactive catalyst coated on industrial porcelain grès tiles to photodegrade drugs in water, *Environ. Sci. Pollut. Res. Int.* (2017) 1–6.
[9] L. He, X. Sun, F. Zhu, S. Ren, S. Wang, OH-initiated transformation and hydrolysis of aspirin in AOPs system: DFT and experimental studies, *Sci. Total Environ.* 592 (2017) 33–40.
[10] M.M. Ismail, T.M. Essam, Y.M. Ragab, A.E. El-Sayed, F.E. Mourad, Remediation of a mixture of analgesics in a stirred-tank photobioreactor using microalgal–bacterial consortium coupled with attempt to valorise the harvested biomass, *Bioresour. Technol.* 232 (2017) 364–371.
[11] S.H. Lee, O.H. Lin, R.A. Doong, Design of size-tunable molecularly imprinted polymer for selective adsorption of acetaminophen, *Clean Techn. Environ. Policy* 19 (1) (2017) 243–250.
[12] L.A. Al-Khateeb, S. Almotiry, M.A. Salam, Adsorption of pharmaceutical pollutants onto graphene nanoplatelets, *Chem. Eng. J.* 248 (2014) 191–199.
[13] K. Mphahlele, M.S. Onyango, S.D. Mhlanga, Adsorption of aspirin and paracetamol from aqueous solution using Fe/N-CNT/beta-cyclodextrin nanocomopsites synthesized via a benign microwave assisted method, *J. Environ. Chem. Eng.* 3 (4) (2015) 2619–2630.
[14] V. Rakic, V. Rac, M. Krmar, O. Otman, A. Auroux, The adsorption of pharmaceutically active compounds from aqueous solutions onto activated carbons, *J. Hazard. Mater.* 282 (2015) 141–149.

[15] I. Anastopoulos, A. Bhatnagar, B.H. Hameed, Y.S. Ok, M. Omirou, A review on waste-derived adsorbents from sugar industry for pollutant removal in water and wastewater, *J. Mol. Liq.* 240 (2017) 179–188.

[16] K.S.A. Sohaimi, N. Ngadi, H. Mat, I.M. Inuwa, S. Wong, Synthesis, characterization and application of textile sludge biochars for oil removal, *J. Environ. Chem. Eng.* 5 (2) (2017) 1415–1422.

[17] S.H. Md Arshad, N. Ngadi, A.A. Aziz, N.S. Amin, M. Jusoh, S. Wong, Preparation of activated carbon from empty fruit bunch for hydrogen storage, *J. Energy Storage* 8 (2016) 257–261.

[18] Z.A. Ghani, M.S. Yusoff, N.Q. Zaman, M. Zamri, J. Andas, Optimization of preparation conditions for activated carbon from banana pseudo-stem using response surface methodology on removal of color and COD from landfill leachate, *Waste Manag.* 62 (2017) 177–187.

[19] T. Mukoko, M. Mupa, U. Guyo, F. Dziike, Preparation of rice hull activated carbon for the removal of selected pharmaceutical waste compounds in hospital effluent, *J. Environ. Anal. Toxicol.* (S7) (2015) 1.

[20] A. Solanki, T.H. Boyer, Pharmaceutical removal in synthetic human urine using biochar, *Environ. Sci.: Water Res. Technol.* 3 (3) (2017) 553–565.

[21] D. Bolton, Global Tea Production 2015, 2016.

[22] C.F. Tang, Y. Shu, R.Q. Zhang, X. Li, J.F. Song, B. Li, Y.T. Zhang, D.L. Ou, Comparison of the removal and adsorption mechanisms of cadmium and lead from aqueous solution by activated carbons prepared from *Typha angustifolia* and *Salix matsudana*, *RSC Adv.* 7 (26) (2017) 16092–16103.

[23] H.N. Tran, H.-P. Chao, S.-J. You, Activated carbons from golden shower upon different chemical activation methods: Synthesis and characterizations, *Adsorpt. Sci. Technol.* 36 (2017) 95–113.

[24] J.Y. Song, B.N. Bhadra, S.H. Jhung, Contribution of H-bond in adsorptive removal of pharmaceutical and personal care products from water using oxidized activated carbon, *Microporous Mesoporous Mater.* 243 (2017) 221–228.

[25] S.L. Goertzen, K.D. Thériault, A.M. Oickle, A.C. Tarasuk, H.A. Andreas, Standardization of the Boehm titration. Part I. CO_2 expulsion and endpoint determination, *Carbon* 48 (4) (2010) 1252–1261.

[26] L. Limousy, I. Ghouma, A. Ouederni, M. Jeguirim, Amoxicillin removal from aqueous solution using activated carbon prepared by chemical activation of olive stone, *Environ. Sci. Pollut. Res. Int.* 24 (11) (2017) 9993–10004.

[27] V. Bernal, A. Erto, L. Giraldo, J.C. Moreno-Pirajan, Effect of solution pH on the adsorption of paracetamol on chemically modified activated carbons, *Molecules* 22 (7) (2017) 1032.

[28] M.A. Yahya, Z. Al-Qodah, C.W.Z. Ngah, Agricultural bio-waste materials as potential sustainable precursors used for activated carbon production: A review, *Renew. Sustain. Energy Rev.* 46 (2015) 218–235.

[29] I.M. Inuwa, A. Hassan, D.Y. Wang, S.A. Samsudin, M.K.M. Haafiz, S.L. Wong, M. Jawaid, Influence of exfoliated graphite nanoplatelets on the flammability and thermal properties of polyethylene terephthalate/polypropylene nanocomposites, *Polym. Degrad. Stab.* 110 (0) (2014) 137–148.

[30] K.S.A. Sohaimi, N. Ngadi, H. Mat, I.M. Inuwa, S. Wong, Synthesis, characterization and application of textile sludge biochars for oil removal, *J. Environ. Chem. Eng.* 5 (2) (2017) 1415–1422.

[31] M. Belhachemi, M. Jeguirim, L. Limousy, F. Addoun, Comparison of NO_2 removal using date pits activated carbon and modified commercialized activated carbon via different preparation methods: Effect of porosity and surface chemistry, *Chem. Eng. J.* 253 (2014) 121–129.

[32] G. Selvaraju, N.K. Abu Bakar, Production of a new industrially viable green-activated carbon from *Artocarpus integer* fruit processing waste and evaluation of its chemical, morphological and adsorption properties, *J. Clean. Prod.* 141 (2017) 989–999.

[33] V. Bernal, L. Giraldo, J.C. Moreno-Piraján, Thermodynamic study of the interactions of salicylic acid and granular activated carbon in solution at different pHs, *Adsorpt. Sci. Technol.* (2017), https://doi.org/10.1177/0263617417730463.

[34] G.M. Santana, R.C.C. Lelis, E.F. Jaguaribe, R.D. Morais, J.B. Paes, P.F. Trugilho, Development of activated carbon from bamboo (*Bambusa vulgaris*) for pesticide removal from aqueous solutions, *Cerne* 23 (1) (2017) 123–131.

[35] M. Auta, B.H. Hameed, Preparation of waste tea activated carbon using potassium acetate as an activating agent for adsorption of Acid Blue 25 dye, *Chem. Eng. J.* 171 (2) (2011) 502–509.

[36] Y. Gokce, Z. Aktas, Nitric acid modification of activated carbon produced from waste tea and adsorption of methylene blue and phenol, *Appl. Surf. Sci.* 313 (Supplement C) (2014) 352–359.

[37] T. Mahmood, R. Ali, A. Naeem, M. Hamayun, M. Aslam, Potential of used *Camellia sinensis* leaves as precursor for activated carbon preparation by chemical activation with H_3PO_4; optimization using response surface methodology, *Process Saf. Environ. Prot.* 109 (2017) 548–563.

[38] A. Gundogdu, C. Duran, H.B. Senturk, M. Soylak, M. Imamoglu, Y. Onal, Physicochemical characteristics of a novel activated carbon produced from tea industry waste, *J. Anal. Appl. Pyrolysis* 104 (2013) 249–259.

[39] S. Roy, P. Das, S. Sengupta, Treatability study using novel activated carbon prepared from rice husk: Column study, optimization using response surface methodology and mathematical modeling, *Process Saf. Environ. Prot.* 105 (2017) 184–193.

[40] F. Guzel, H. Saygili, G.A. Saygili, F. Koyuncu, C. Yilmaz, Optimal oxidation with nitric acid of biochar derived from pyrolysis of weeds and its application in removal of hazardous dye methylene blue from aqueous solution, *J. Clean. Prod.* 144 (2017) 260–265.

[41] O.A. Ekpete, A.C. Marcus, V. Osi, Preparation and characterization of activated carbon obtained from plantain (*Musa paradisiaca*) fruit stem, *J. Chem.* 2017 (2017), 8635615.

[42] I. Ghouma, M. Jeguirim, S. Dorge, L. Limousy, C.M. Ghimbeu, A. Ouederni, Activated carbon prepared by physical activation of olive stones for the removal of NO_2 at ambient temperature, *C. R. Chim.* 18 (1) (2015) 63–74.

[43] K.S. Sing, Reporting physisorption data for gas/solid systems with special reference to the determination of surface area and porosity (Recommendations 1984), *Pure Appl. Chem.* 57 (4) (1985) 603–619.

[44] M. Dutta, U. Das, S. Mondal, S. Bhattachriya, R. Khatun, R. Bagal, Adsorption of acetaminophen by using tea waste derived activated carbon, *Int. J. Environ. Sci.* 6 (2) (2015) 270.

[45] N.Y. Yahya, N. Ngadi, I.I. Muhamad, H. Alias, Application of cellulose from pandan leaves as grafted flocculant for dyes treatment, *J. Eng. Sci. Technol.* 10 (2015) 19–28.

[46] J. Wang, F.A. Wu, M. Wang, N. Qiu, Y. Liang, S.Q. Fang, X. Jiang, Preparation of activated carbon from a renewable agricultural residue of pruning mulberry shoot, *Afr. J. Biotechnol.* 9 (19) (2010) 2762–2767.

[47] A. Gundogdu, C. Duran, H.B. Senturk, M. Soylak, D. Ozdes, H. Serencam, M. Imamoglu, Adsorption of phenol from aqueous solution on a low-cost activated carbon produced from tea industry waste: Equilibrium, kinetic, and thermodynamic study, *J. Chem. Eng. Data* 57 (10) (2012) 2733–2743.

[48] I.I. Gurten, M. Ozmak, E. Yagmur, Z. Aktas, Preparation and characterisation of activated carbon from waste tea using K_2CO_3, *Biomass Bioenergy* 37 (2012) 73–81.

[49] S. Beninati, D. Semeraro, M. Mastragostino, M. Mastragostino, Adsorption of paracetamol and acetylsalicylic acid onto commercial activated carbons, *Adsorpt. Sci. Technol.* 26 (9) (2008) 721–734.

[50] C.S. Gulipalli, B. Prasad, K.L. Wasewar, Batch study, equilibrium and kinetics of adsorption of selenium using rice husk ash (RHA), *J. Eng. Sci. Technol.* 6 (5) (2011) 586–605.

[51] N. Nasuha, B.H. Hameed, A.T. Din, Rejected tea as a potential low-cost adsorbent for the removal of methylene blue, *J. Hazard. Mater.* 175 (1-3) (2010) 126–132.

[52] T. Sumathi, G. Alagumuthu, Adsorption studies for arsenic removal using activated *Moringa oleifera*, *Int. J. Chem. Eng.* 2014 (2014), 430417.

[53] P.M.K. Reddy, P. Verma, C. Subrahmanyam, Bio-waste derived adsorbent material for methylene blue adsorption, *J. Taiwan Inst. Chem. Eng.* 58 (2016) 500–508.

[54] S. Wong, N.A.N. Yac'cob, N. Ngadi, O. Hassan, I.M. Inuwa, From pollutant to solution of wastewater pollution: Synthesis of activated carbon from textile sludge for dyes adsorption, *Chin. J. Chem. Eng.* 26 (4) (2018) 870–878.

[55] A.W. Adamson, A.P. Gast, Physical Chemistry of Surfaces, Sixth ed. John Wiley & Sons, Inc., 1967

[56] B. Wanassi, I.B. Hariz, C.M. Ghimbeu, C. Vaulot, M.B. Hassen, M. Jeguirim, Carbonaceous adsorbents derived from textile cotton waste for the removal of Alizarin S dye from aqueous effluent: Kinetic and equilibrium studies, *Environ. Sci. Pollut. Res. Int.* 24 (11) (2017) 10041–10055.

[57] P.S. Ardekani, H. Karimi, M. Ghaedi, A. Asfaram, M.K. Purkait, Ultrasonic assisted removal of methylene blue on ultrasonically synthesized zinc hydroxide nanoparticles on activated carbon prepared from wood of cherry tree: Experimental design methodology and artificial neural network, *J. Mol. Liq.* 229 (2017) 114–124.

[58] Ş. Parlayıcı, E. Pehlivan, Removal of metals by Fe_3O_4 loaded activated carbon prepared from plum stone (*Prunus nigra*): Kinetics and modelling study, *Powder Technol.* 317 (2017) 23–30.

[59] A. Dada, A. Olalekan, A. Olatunya, O. Dada, Langmuir, Freundlich, Temkin and Dubinin–Radushkevich isotherms studies of equilibrium sorption of Zn^{2+} unto phosphoric acid modified rice husk, *IOSR J. Appl. Chem.* 3 (1) (2012) 38–45.

[60] N. Chaukura, W. Gwenzi, N. Mupatsi, D.T. Ruziwa, C. Chimuka, Comparative adsorption of Zn^{2+} from aqueous solution using hydroxylated and sulphonated biochars derived from pulp and paper sludge, *Water Air Soil Pollut.* 228 (1) (2016) 7.

[61] S. Alvarez-Torrellas, M. Martin-Martinez, H.T. Gomes, G. Ovejero, J. Garcia, Enhancement of p-nitrophenol adsorption capacity through N-2-thermal-based treatment of activated carbons, *Appl. Surf. Sci.* 414 (2017) 424–434.

[62] B.H. Hameed, D.K. Mahmoud, A.L. Ahmad, Equilibrium modeling and kinetic studies on the adsorption of basic dye by a low-cost adsorbent: Coconut (*Cocos nucifera*) bunch waste, *J. Hazard. Mater.* 158 (1) (2008) 65–72.

[63] P. Maneechakr, S. Karnjanakom, Adsorption behaviour of Fe(II) and Cr(VI) on activated carbon: Surface chemistry, isotherm, kinetic and thermodynamic studies, *J. Chem. Thermodyn.* 106 (2017) 104–112.

[64] A.B. Fadhil, Evaluation of apricot (*Prunus armeniaca* L.) seed kernel as a potential feedstock for the production of liquid bio-fuels and activated carbons, *Energy Convers. Manag.* 133 (2017) 307–317.